Electronic Supplementary Material (ESI) for Chemical Communications.
This journal is © The Royal Society of Chemistry 2022

Supporting Information

Tumor microenvironment responsive S-NSs-TPZ-ICG intelligent nanoplatform for synergistically enhanced tumor multimodal therapy

Xiangcao Li,[a] Shaojing Zhao,[a] Ke Yang,[a] Baoling Li,[a] Benhua Wang,[a] Jianing Yi,[b] Xiangzhi Song,[a] and Minhuan Lan*[a]*

[a] Key Laboratory of Hunan Province for Water Environment and Agriculture Product Safety, College of Chemistry and Chemical Engineering, Central South University, Changsha, 410083, P. R. China. E-mail: minhuanlan@csu.edu.cn

[b] Surgical Department of Breast and Thyroid Gland, Hunan Provincial People's Hospital, the First Affiliated Hospital of Hunan Normal University, Changsha, Hunan, 410005, P. R. China. E-mail: yijianing@hunnu.edu.cn

Experimental Section

Materials

Indocyanine green (ICG) was purchased from Energy Chemical. Singlet Oxygen Sensor Green (SOSG) was purchased from Dalian Meilun Biotechnology Co., Ltd. Calcein acetoxymethylester (Calcine AM), propidium iodide (PI), and 3-(4,5-dimethylthiazol-2-yl)-2,5-diphenyltetrazolium bromide (MTT) were purchased from Tianjin Heans Biochemical Technology Co., Ltd. Roswell Park Memorial Institute-1640 (RPMI-1640), Dulbecco's modified eagle medium (DMEM), and PBS (phosphate buffer saline) were purchased from Wuhan saiweier Biotechnology Co., Ltd. Fetal bovine serum was purchased from Thermo Fisher Scientific. 2′,7′-dichlorofluorescein diacetate (DCFH-DA) was purchased from Shanghai McLean Biochemical Technology Co., Ltd.

Instrumentation

Atomic force microscopy (AFM) images were recorded using a Nano-Scope (Bruker). Transmission electron microscopy (TEM) images were obtained using a JEOL JEM-2100F electron microscope. Fourier transform infrared spectroscopy (FT-IR) spectra were acquired using an M15E-PS/10 (Bruker) IR spectrometer. Absorption and fluorescence spectra were measured using Shimadzu UV-2600 and RF-6000 spectrophotometers, respectively. Zeta potentials were quantified on the zeta-sizer Nano-ZS (Malvern). The fluorescence imaging was performed on a Leica SP8 confocal laser scanning microscopy.

Preparation of S-NSs

0.50 g of sulfur powder was added to 50 mL of ultrapure water containing 5 mg of bovine serum albumin (BSA). The mixture was then sonicated for 20 min using a cell disruptor. The supernatant was collected after centrifugation, and dialyzed using a 3500 Da dialysis membrane for 24 h.

Preparation of S-NSs-TPZ-ICG

5 mL of S-NSs solution, 3 mL of ICG (0.01 mg/mL), and 2 mL of TPZ (0.01 mg/mL) solution were mixed in a round-bottomed flask. The solution was then allowed to react for 24 h under constant stirring. Finally, the reaction solution was purified by dialysis to obtain **S-NSs-TPZ-ICG**.

Photodynamic performance of S-NSs-TPZ-ICG

SOSG was used to detect the generation of singlet oxygen from a water solution. **S-NSs-TPZ-ICG** (90 μg/mL) was mixed with SOSG (2.5 μM) and then irradiated (λ_{ex}=808 nm; 1 W/cm^2) for 90 s. The fluorescence of oxidized SOSG (λ_{ex}=504 nm; λ_{em}=525 nm) was then recorded every 30 s.

MTT assay

4T1 cells were cultivated in Roswell Park Memorial Institute-1640 (RPMI-1640) medium containing 1% antibiotics and 10% fetal bovine serum (FBS). The cells were cultured at 37 ℃ in a humidified atmosphere containing 5% CO_2.

Intracellular ROS assay

DCFH-DA was used as an indicator to detect intracellular ROS generation. **S-NSs-TPZ-ICG** was added 4 h before laser irradiation, and DCFH-DA was added 30 min before laser irradiation. After irradiation with an 808 nm laser (1 W/cm^2, 10 min), the confocal disk was washed three times with PBS. The fluorescence images were captured by confocal laser scanning microscopy (Leica SP8).

PTT/PDT treatment of cancer cells

4T1 cells were cultivated in confocal dishes in RPMI-1640 medium overnight. Individual dishes were then processed as follows: PBS only; PBS + laser; S-NSs-TPZ; **S-NSs-TPZ-ICG**; and **S-NSs-TPZ-ICG** + laser. After treatment, the cells were stained with Calcein-AM (10 μg/mL) and PI (5 μg/mL). Finally, fluorescence images were captured by confocal laser scanning microscopy (Leica SP8).

Animal model

Animal care and experiments were performed in compliance with Animal Care and Institutional Ethical Guidelines in China. In accordance with Animal Research Ethics Committee of Central South University, and the committee has approved our experiments, permit number SCXK (Hunan) 2019-0004. All the animal experiments complied with relevant guidelines of the Chinese government and regulations for the care and use of experimental animals. The mice (8-week-old BALB/c males) were purchased from Hunan SJA Laboratory Animal Co., Ltd. To establish the mouse tumor model, 4T1 cells were subcutaneously administered into the mice.

***In vivo* NIR-I imaging**

Once the tumors in the 4T1 tumor-bearing mice had reached approx. 150 mm^3, 100 μL of **S-NSs-TPZ-ICG** (90 μg/mL) aqueous solution was intratumorally injected. Next, real-time *in vivo* NIR-I imaging was performed using a Near infrared InGaAs array imaging detector (λ_{ex}=808 nm; 1 W/cm^2).

***In vivo* treatment**

The *in vivo* therapeutic effect of **S-NSs-TPZ-ICG** was assessed after the 4T1 tumor volume had reached approx. 100 mm^3. Mice were randomly divided into PBS, PBS+laser, **S-NSs-TPZ-ICG**, and **S-NSs-TPZ-ICG** + laser groups. The mice were then anesthetized and irradiated with an 808 nm laser for 10 min (1 W/cm^2). Subsequently, changes in mouse body weight and tumor volume were measured and recorded for 21 days. The mouse tumors were then processed with Ki67 and H&E staining.

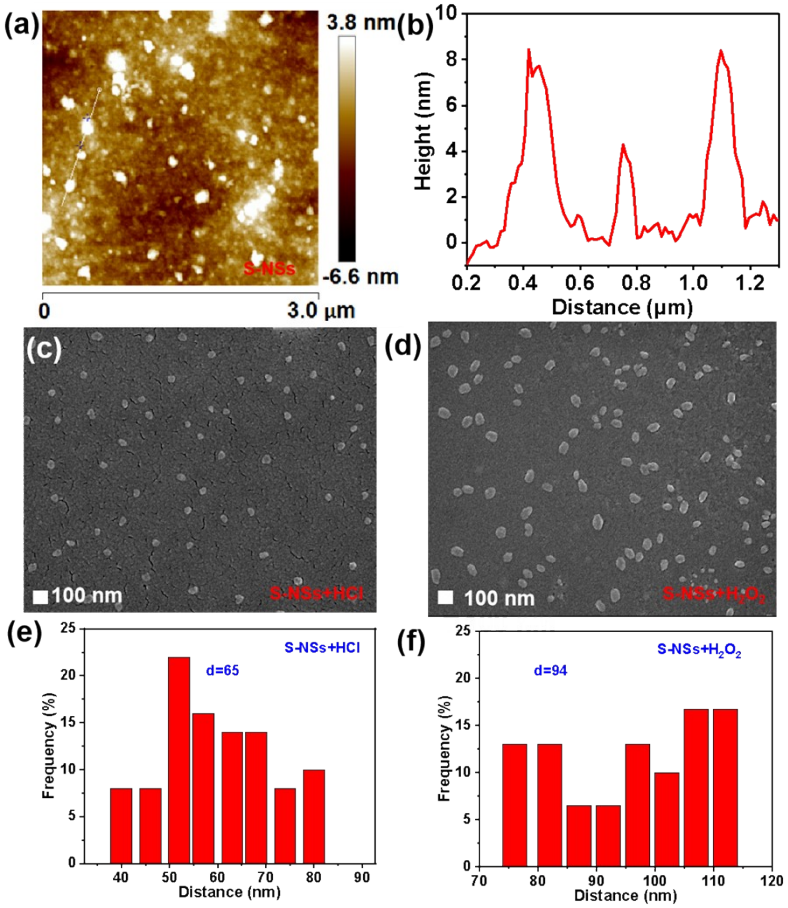

Fig. S1. (a) AFM image of S-NSs. (b) Section analysis of AFM image; (c, d) SEM images and (e, f) size distribution of S-NSs in the presence of (c, e) HCl (pH 5.5) and (d, f) H_2O_2 (100 uM), respectively.

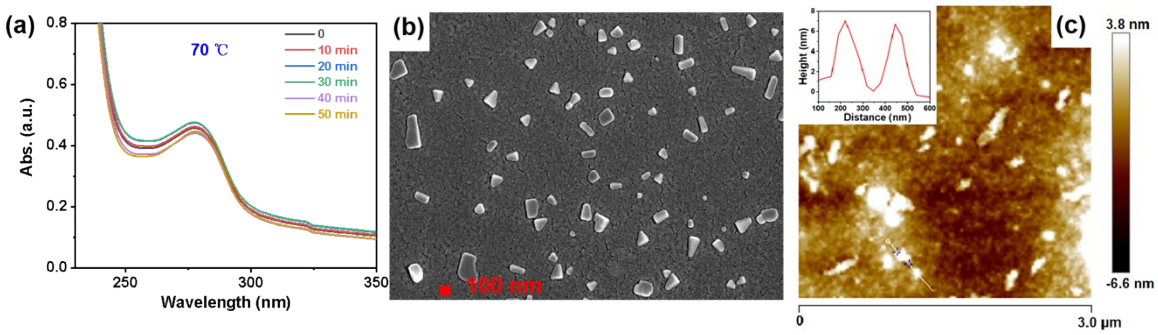

Fig. S2. (a) Heating time-dependent UV-vis absorption spectra of S-NSs at 70℃. (b) SEM and (c) AFM images of S-NSs under 70 ℃ heating for 50 min.

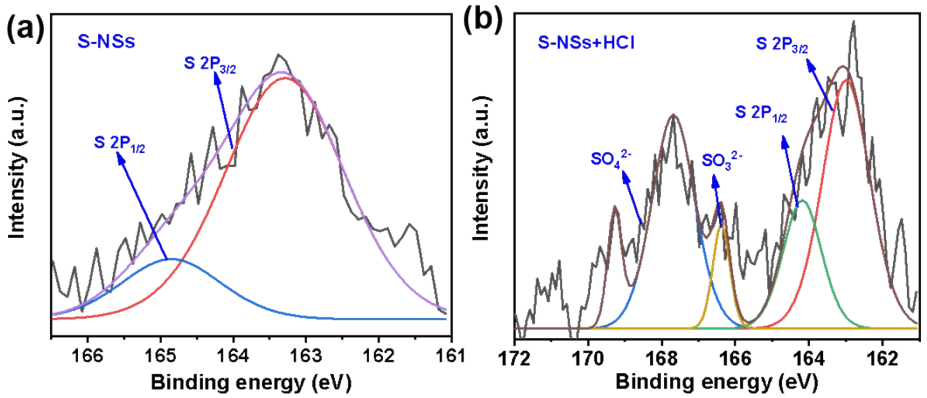

Fig. S3. The deconvoluted high resolution XPS spectra of S2p of S-NSs in the (a) absence and (b) presence of HCl (pH 5.5).

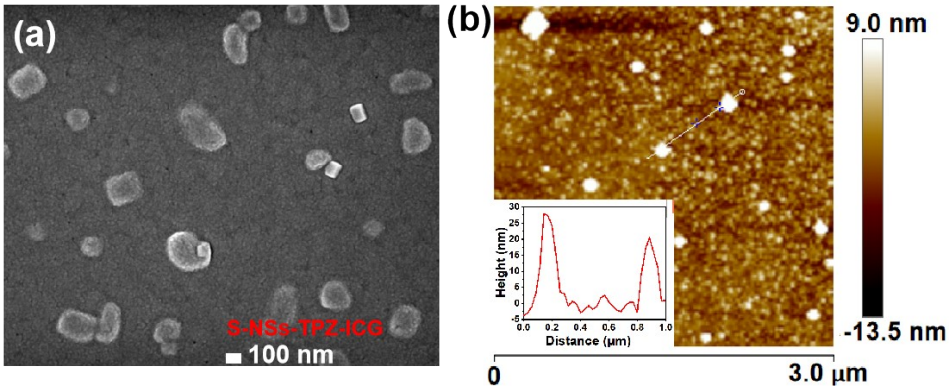

Fig. S4. (a) SEM and (b) AFM images of S-NSs-TPZ-ICG. The inset in (b) is the section analysis of AFM image.

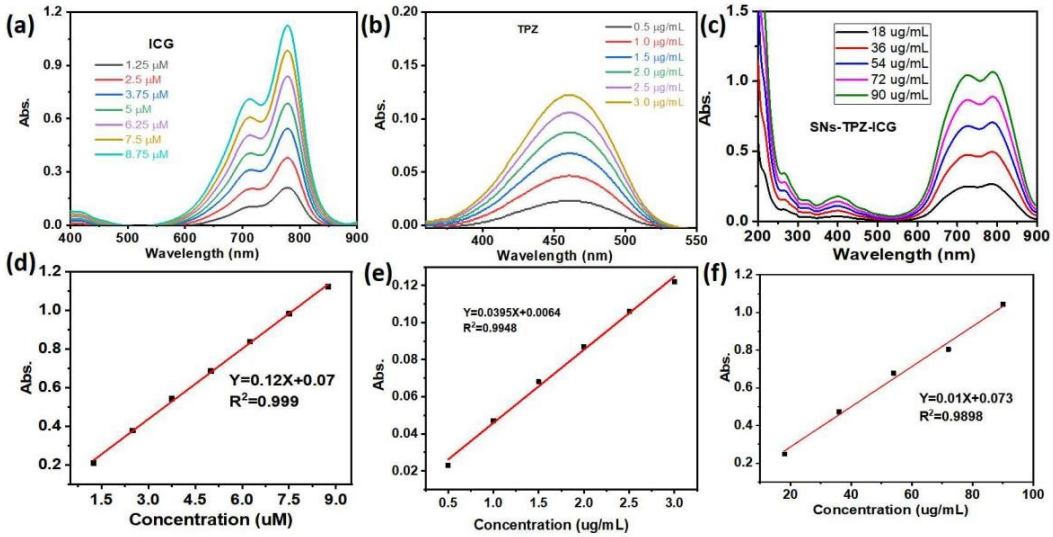

Fig. S5. (a-c) The UV-vis absorption spectra of ICG, TPZ, and S-NSs-TPZ-ICG with different concentration, and (d-f) the corresponding linearship between the absorbance and concentration of the sample. The loading efficiency of ICG and TPZ is calculated to be 94% and 6.3%, respectively.

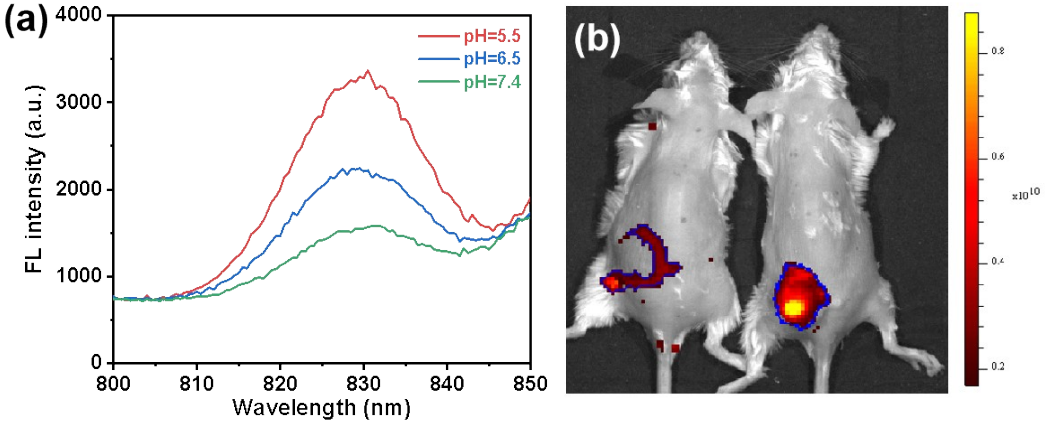

Fig. S6. (a) Fluorescent spectra of S-NSs-TPZ-ICG aqueous solution with different pH value. (b) *In vivo* fluorescent images of the mice tumor-injected (right) and normal tissue-injected (left) with S-NSs-TPZ-ICG aqueous solution.

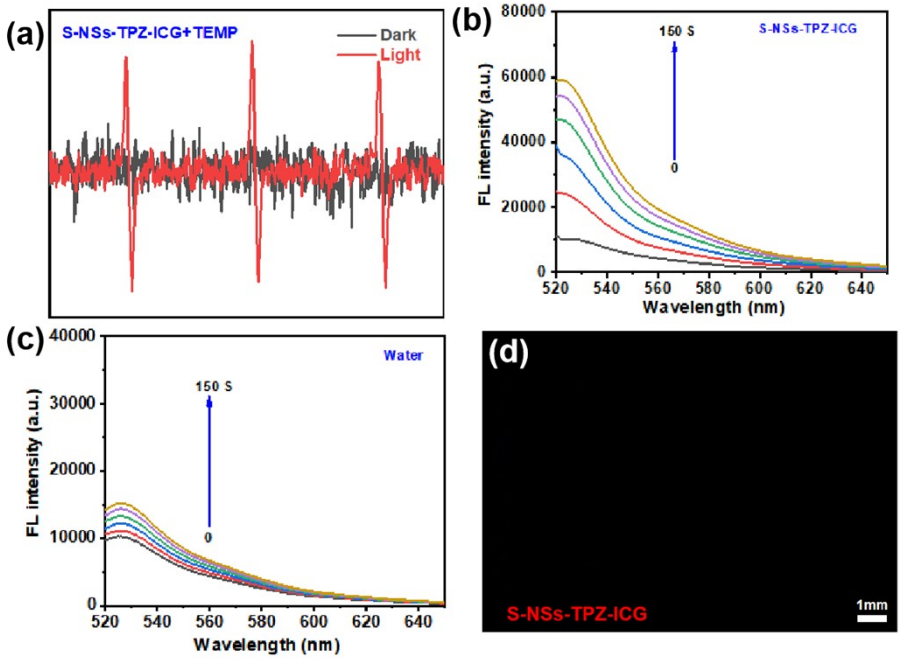

Fig. S7. (a) EPR spectra of S-NSs-TPZ-ICG aqueous solution under dark (black line) or laser irradiation (red line). Time-dependent fluorescent spectra (Ex: 504 nm) of (b) S-NSs-TPZ-ICG (90 μg/mL) and (c) water in the presence of SOSG under 808 nm laser irradiation; (d) Fluorescent images of 4T1 cells incubated with S-NSs-TPZ-ICG and DCFH.

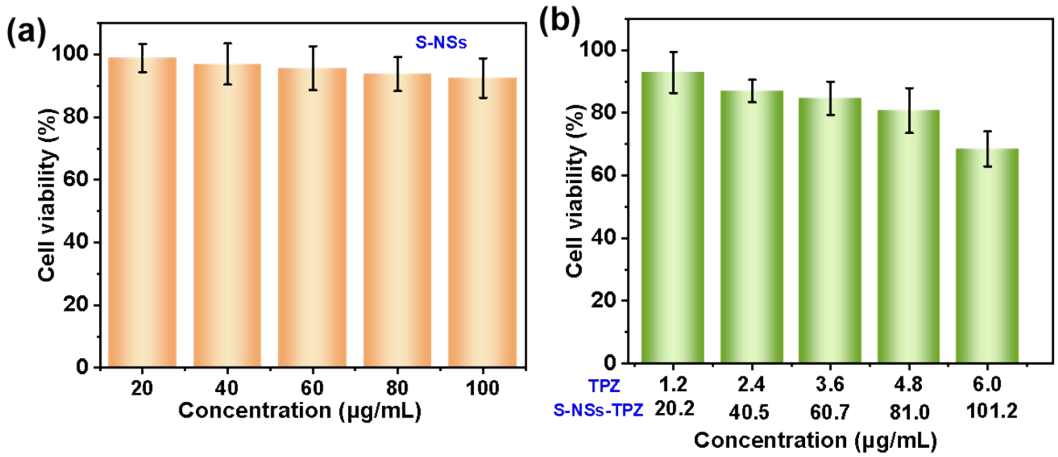

Fig. S8. Viability of 4T1 cells incubated with different concentrations of (a) S-NSs and (b) S-NSs-TPZ in the dark.

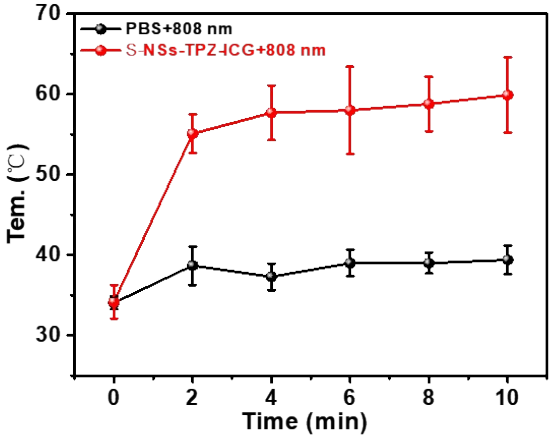

Fig. S9. Irradiation time dependent-temperature change at tumor site after treatment with PBS + laser or S-NSs-TPZ-ICG + laser.

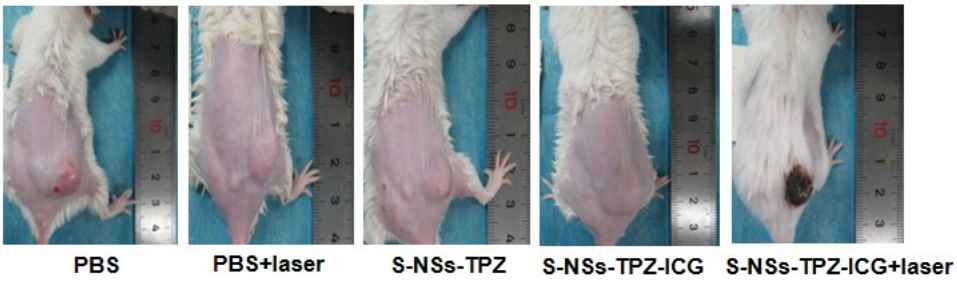

Fig. S10. Photos of tumor-bearing mice after 14 days of treatment.

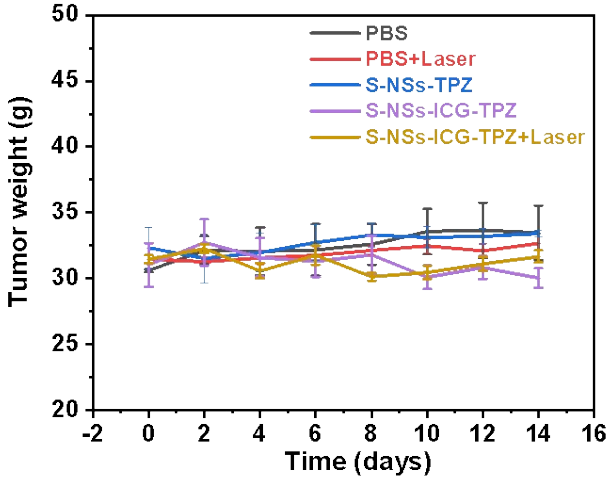

Fig. S11. Body weight change of the mice over the treatment course.